Clinical Translation of Hyperpolarized ^{13}C Pyruvate and Urea MRI for Simultaneous Metabolic and Perfusion Imaging

Supporting Information

Hecong Qin[1,2], Shuyu Tang[1, †], Andrew M. Riselli[1], Robert A. Bok[1], Romelyn Delos Santos[1], Mark van Criekinge[1], Jeremy W. Gordon[1], Rahul Aggarwal[3], Rui Chen[4], Gregory D. Goddard[5], Chunxin Tracy Zhang[5], Albert Chen[4], Galen Reed[4], Daniel M. Ruscitto[4], James Slater[1], Renuka Sriram[1], Peder E. Z. Larson[1,2], Daniel B. Vigneron[1,2], John Kurhanewicz[1,2, *]

1. Department of Radiology and Biomedical Imaging, University of California, San Francisco, San Francisco, CA

2. Graduate Program in Bioengineering, University of California, Berkeley and San Francisco, San Francisco, CA

3. Department of Medicine, University of California, San Francisco, San Francisco, CA

4. General Electric Healthcare, Milwaukee, WI

5. General Electric Research, Niskayuna, NY

†. Current address: HeartVista Inc., Los Altos, CA, USA

* Corresponding author:

John Kurhanewicz, Ph.D.

Professor of Radiology and Biomedical Imaging, Urology, and Pharmaceutical Chemistry

University of California, San Francisco

1700 4th St, BH 203E

San Francisco, CA 94143

E-mail: John.Kurhanewicz@ucsf.edu

I. Differential Scanning Calorimetry (DSC) Methods and Results.

A TA instrument Q2000 DSC (New Castle, DE) was used. The sample was loaded at room temperature, then heated to 40 °C and remained isothermal at 40 °C for 30 minutes. The system is then cooled to -90 °C and remained isothermal at -90 °C for 5 minutes, before heating to 40 °C again and remaining isothermal at 40 °C for 30 minutes to ensure complete sample melting. The above process was repeated twice for each sample. For all heating and cooling steps, a ramp rate of 5°C/min was used. The heat flow (W/g) was recorded during the above thermal transitions (**Figure S.1, S.2**), which demonstrated that pyruvic acid (PA) and urea mixture with 4:1 molar ratio has good glass formation ability and similar glass transition temperature (T_g) to near PA (**Figure S.3, S.4**). No crystallization was observed for the 4:1 PA/urea molar ratio during the thermal cycle from 40 °C to -90 °C.

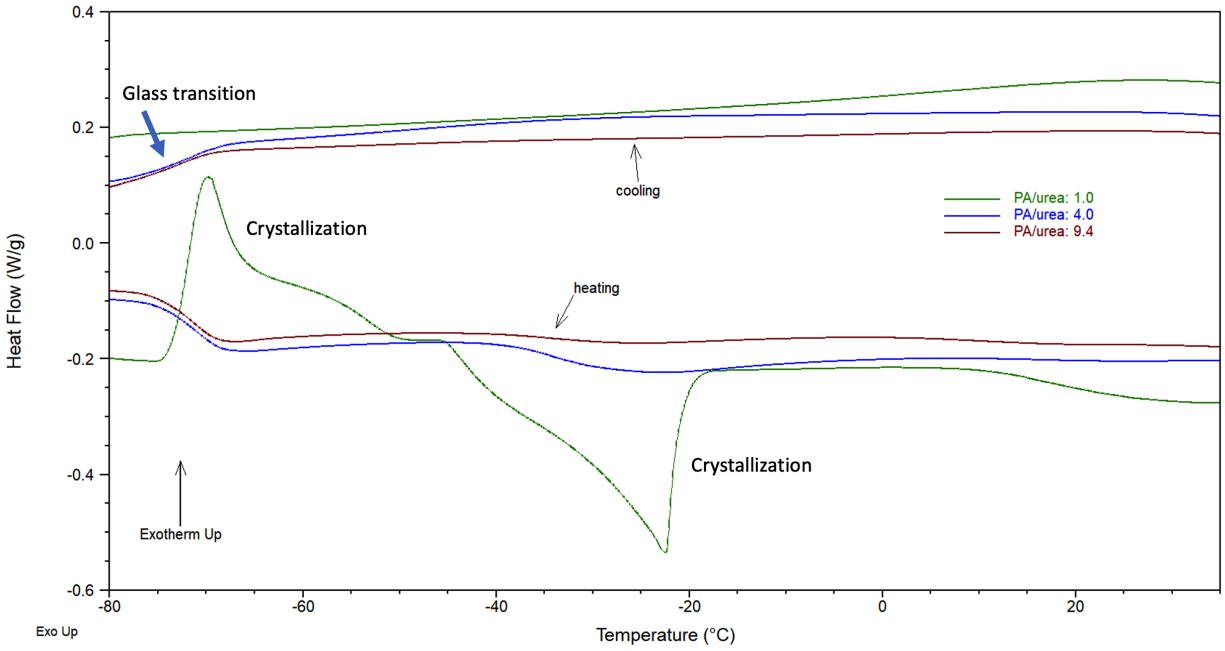

Figure S.1: Heat flow plot of Differential Scanning Calorimetry (DSC) studies on pyruvic acid (PA) and urea mixture: the 4:1 and 9.4:1 PA/urea molar ratios showed similar glass formation around -70°C and no crystallization during the thermal cycle (heating and cooling processes). In contrast, 1:1 PA/urea ratio, which has more water content compared to the other two formulations, showed crystallizations around -70°C and -20°C during the heating process.

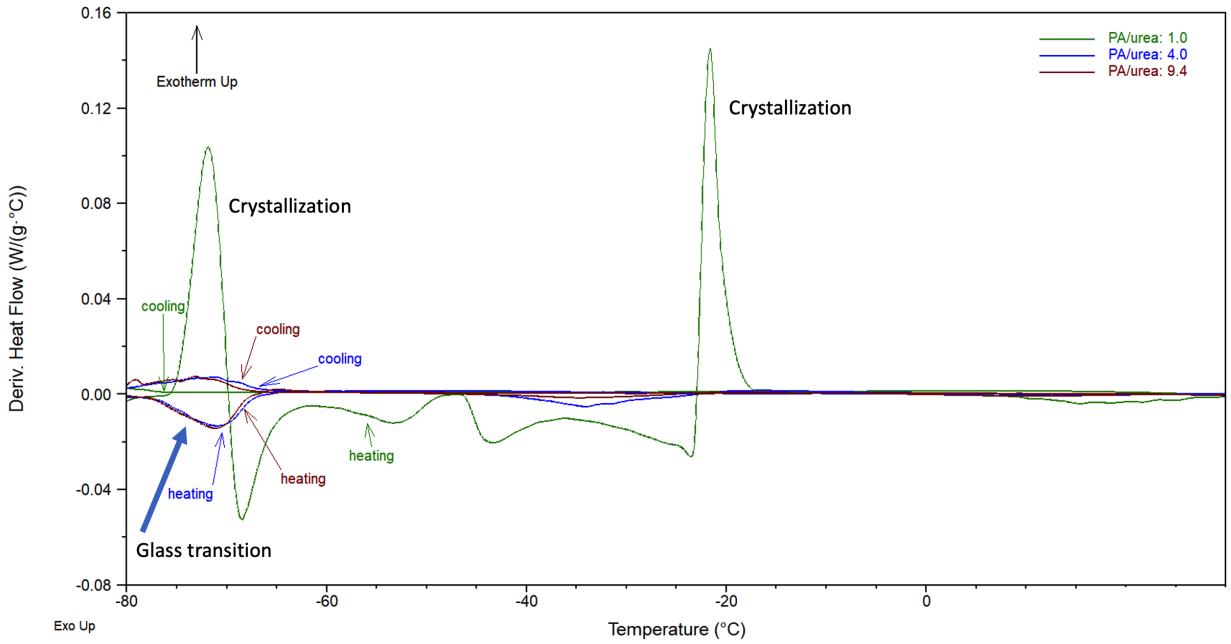

Figure S.2: Heat flow derivative plot of Differential Scanning Calorimetry (DSC) studies on pyruvic acid (PA) and urea mixture: the 4:1 and 9.4:1 PA/urea molar ratios showed similar glass formation around -70°C and no crystallization during the thermal cycle (heating and cooling processes). In contrast, 1:1 PA/urea ratio, which has more water content compared to the other two formulations, showed crystallizations around -70°C and -20°C during the heating process.

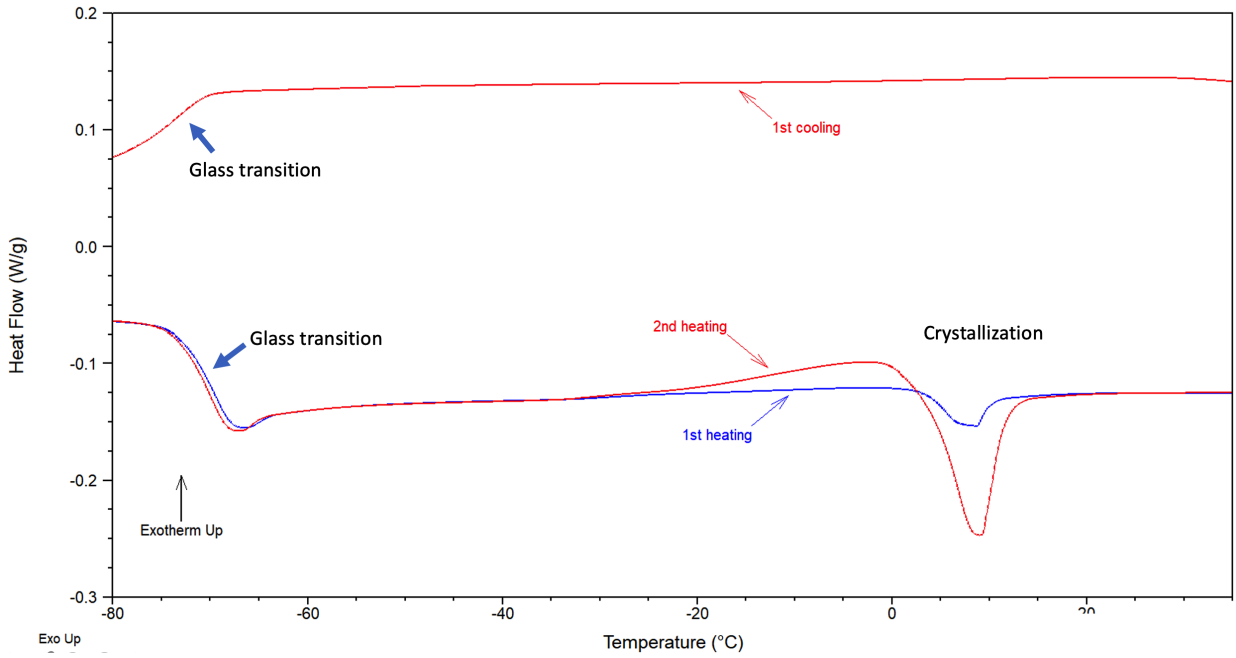

Figure S.3: Heat flow plot of Differential Scanning Calorimetry (DSC) studies on neat pyruvic acid shows glass transitions around -70°C during the thermal cycle (heating and cooling processes), as well as crystallization around 10°C during the heating process.

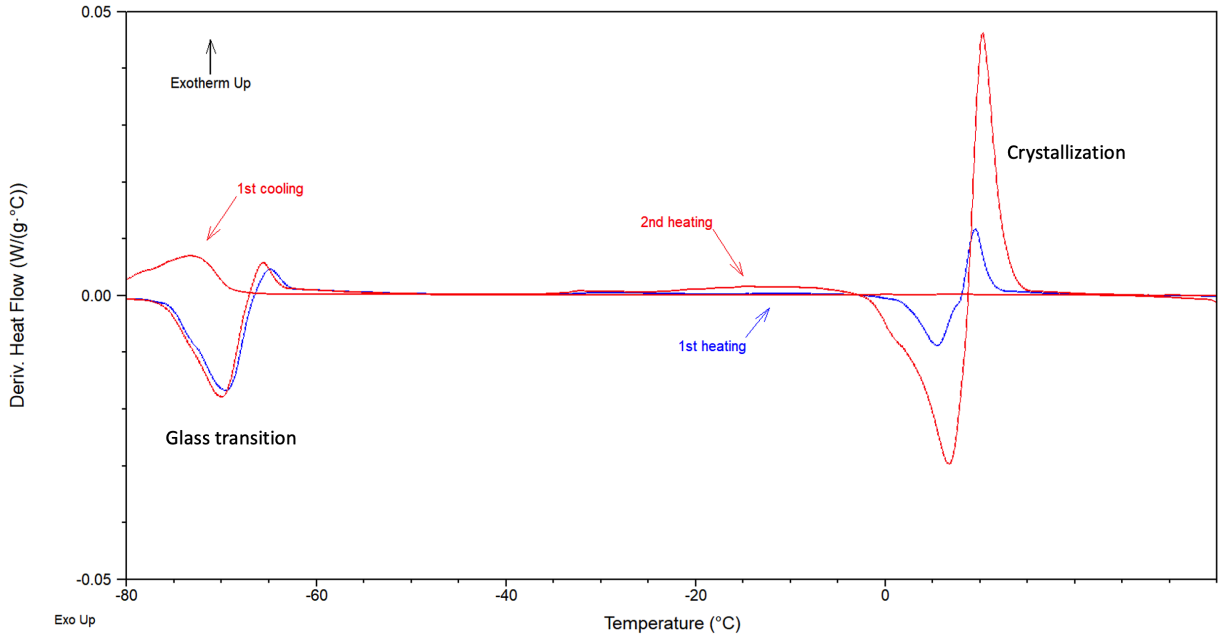

Figure S.4: Heat flow derivative plot of Differential Scanning Calorimetry (DSC) studies on neat pyruvic acid shows glass transitions around -70°C during the thermal cycle (heating and cooling processes), as well as crystallization around 10°C during the heating process.

II. Standard Operation Procedure (SOP) Development and Validation

A set of experiments were performed to optimize and validate the procedures to produce sterile co-polairzed [1-^{13}C]pyruvate and [^{13}C, $^{15}N_2$]urea injection product.

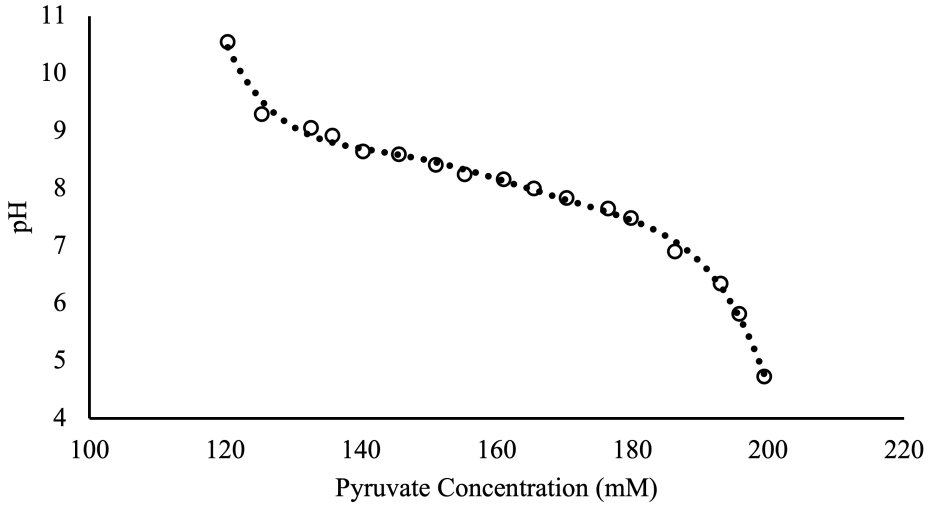

Figure S.5: Validation of the buffer capacity of neutralization media in a titration experiment: the buffer system can neutralize a wide range of pyruvic acid concentration, an experimental variability depending on the sample recovery rate.

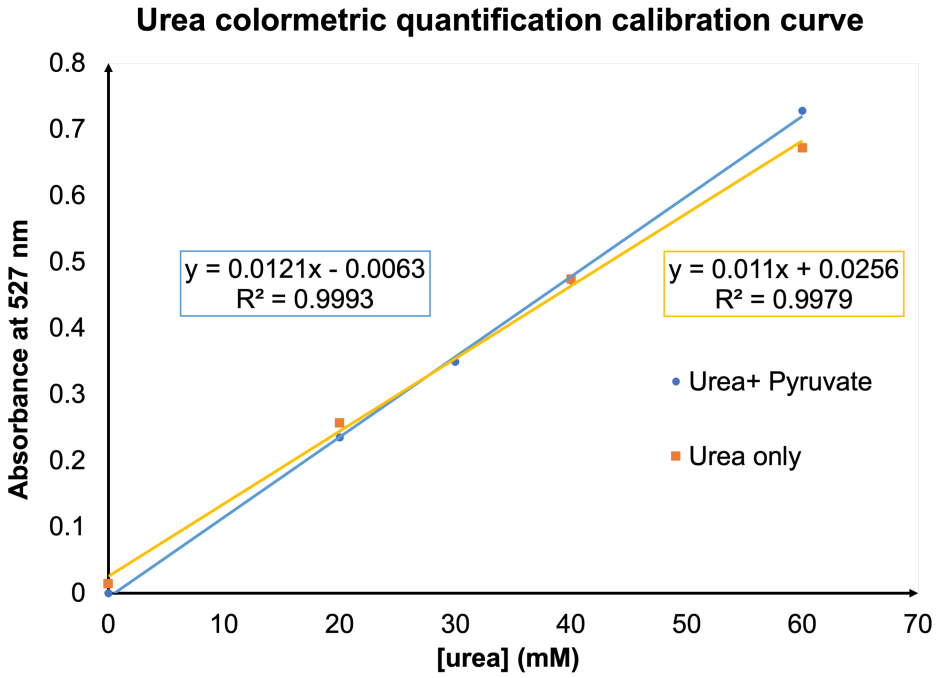

Figure S.6: The linear calibration curve for urea concentration quantification using optical absorbance methods. Urea reacts with 4-(Dimethylamino)cinnamaldehyde (DMAC) at the presence of p-Toluenesulfonic acid and forms a compound with unique absorbance at 525-529 nm. The presence of pyruvate (4:1 pyruvate to urea ratio) has minimal perturbation to urea concentration quantification between 20 to 40 mM (two lines nearly overlap), the target range of urea concentration in the co-polarized injection product.

Table S.1: Process Qualification (PQ) trials for co-polarized [1-^{13}C]pyruvate and [^{13}C, $^{15}N_2$]urea production

Trial	Pyruvate QC (mM)	Urea indirect QC (mM)	Urea validation (mM)	pH	EPA (µM)	Temp (°C)	Volume (ml)	Pyruvate polarization	Urea polarization	Sterility test
1	165	35	33.7	8.05	0.4	34.7	> 40	34.7 %	35.9 %	pass
2	151	34	34.3	8.17	0.7	34.4	> 40	36.6%	38.0%	pass
3	139	32	33.7	8.29	0.9	34	> 40	47.3%	47.9%	pass
4	166	37	43.0	7.7	1.5	37.5	> 40	40.9%	39.1%	pass

Process Qualification (PQ) trials to validate the Standard Operating Procedure (SOP) for routine on-site imaging probe production. The SPINlab quality control (QC) system reports pyruvate concentration, pH, electron paramagnetic agent (EPA) concentration, temperature, and volume. Ratiometric (indirect QC) quantification of urea was performed and found to be in agreement with measurements by photospectrometric method (validation). Percentage polarizations for pyruvate and urea were measured by ^{13}C NMR spectroscopy on a 1.41 T bench-top system. Sterility was assessed by manual integrity tests of the terminal sterility filter and endotoxin tests. All QC metrics for four trials met the pre-defined release criteria.

Table S.2: Quality Control (QC) tests for hyperpolarized [1-^{13}C]pyruvate and [^{13}C,^{15}N$_2$]urea injection product

Test	**Analytical method**	**Target range**
Pyruvate concentration	UV absorbance	125–195 mM
Residual trityl radical (AH 111501) concentration	Visible absorbance	5 µM
pH	Visible absorbance of ratiometric indicators	5.0–9.0
Drug product temperature*	IR pyrometry	25.0–40.0 °C
Drug product volume	Capacitive sensing	$>$ 38 ml
Filter Integrity	Bubble point test	Manufacturer specification

*Specification to temperature is at the time of analysis.

III. NMR impurity analysis

Three sets of ^{13}C NMR experiments were performed on 11.7T/500MHz systems (Bruker Avance III or Varian Inova) to identify and quantify novel impurities in the co-polarized [1-^{13}C]pyruvate and [^{13}C,$^{15}N_2$]urea injection product: 1) **individual raw material** ([^{13}C]urea, [^{13}C,$^{15}N_2$]urea, and [1-^{13}C]pyruvic acid) for baseline structure elucidation and peak assignment (**Figure S.7**); 2) **starting material** of co-polarization (high-concentration, cryovial condition) for impurity identification: neat [1-^{13}C]pyruvic acid mixed with [^{13}C]urea, or [^{13}C,$^{15}N_2$]urea, at 4:1 molar ratio for 60 minutes at room temperature (**Figure 8**); 3) **manual dissolution product** (patient injection condition) for impurity quantification: neutralized [1-^{13}C]pyruvate and [^{13}C,$^{15}N_2$]urea solution. All experiments used D_2O solvent for improved spectral resolution and quality and 1% v/v Gd-DTPA (Magnevist®, Bayer, Whippany, NJ) to ensure spins are fully relaxed. Standard data acquisition parameters were used, including a 5 s repetition time with inverse gated ^{1}H-^{13}C decoupling.

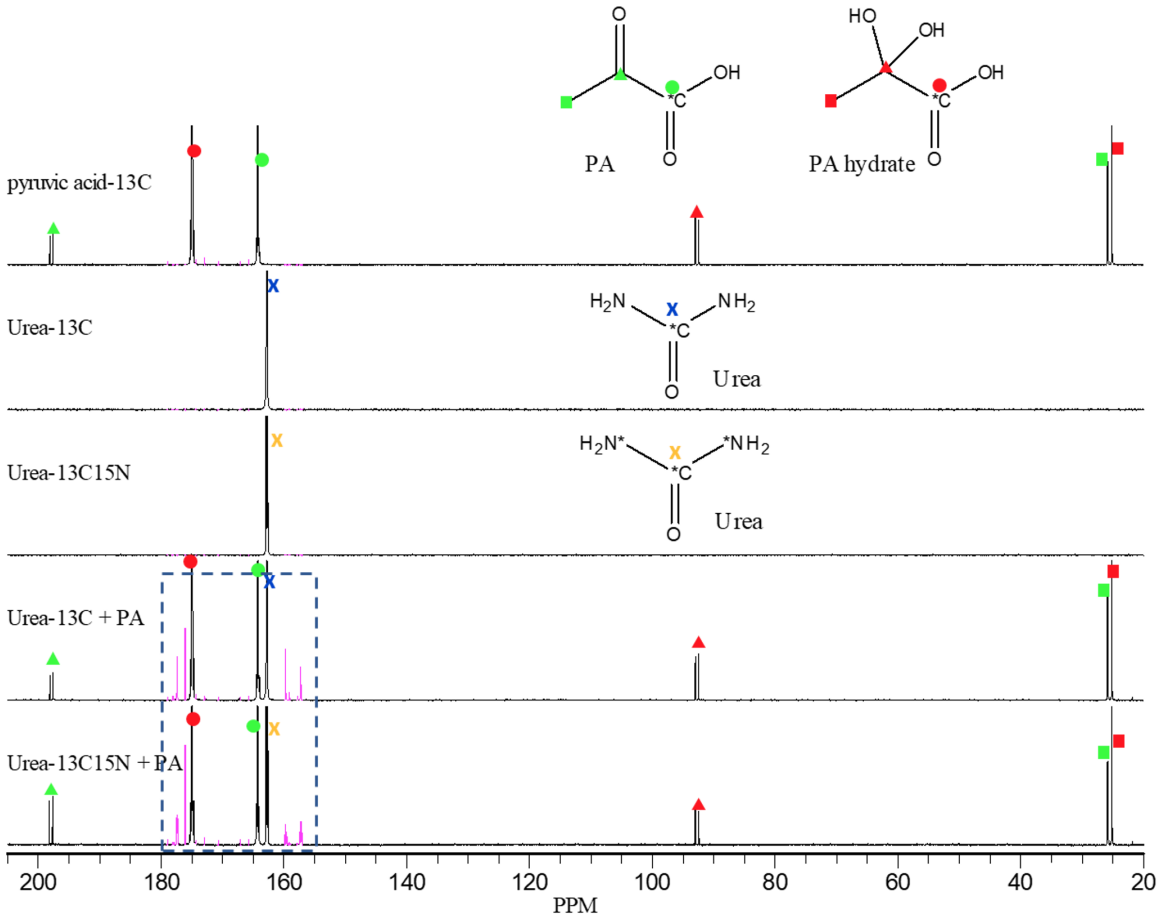

Figure S.7: ^{13}C NMR spectra of raw material and starting material of co-polarization of ^{13}C labeled pyruvic acid (PA) and urea. Peak assignments for PA and PA hydrate were confirmed.

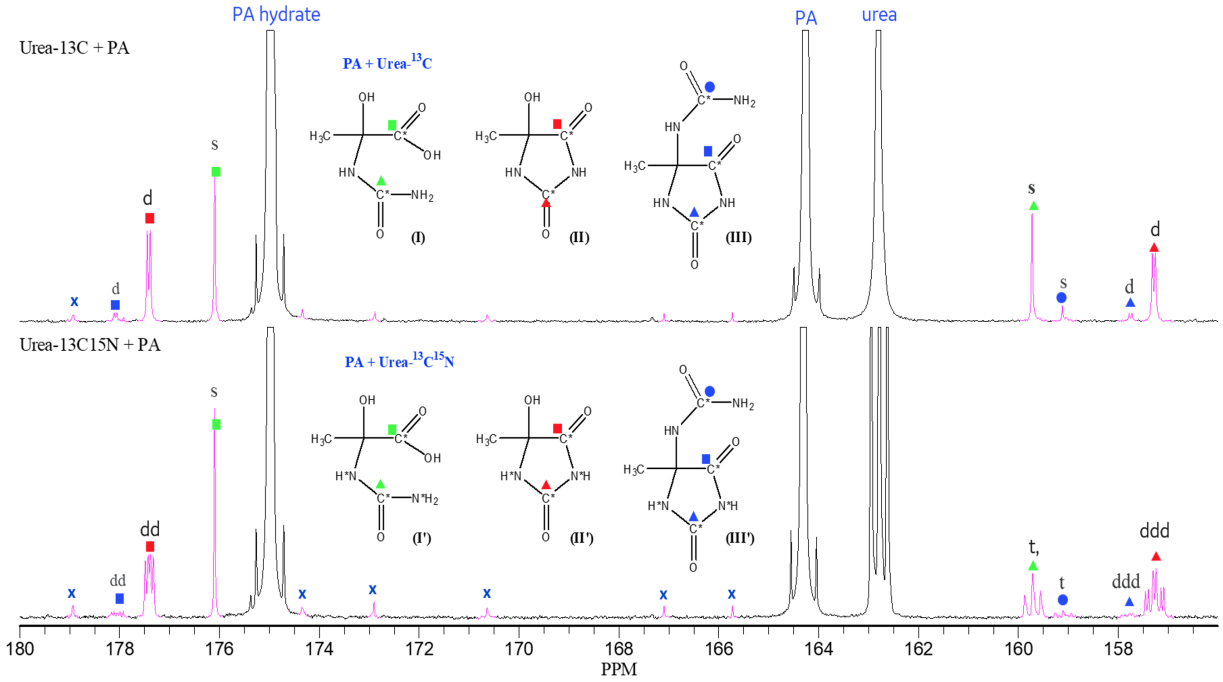

Figure S.8: ^{13}C NMR spectra of [1-^{13}C]pyruvic acid (PA) mixed with [^{13}C]urea and [^{13}C,^{15}N$_2$]urea, respectively (starting material, high concentration cryovial condition). Three novel impurities were shown with peak assignment. Small peaks denoted with "x" corresponds to impurities in the PA raw material.

In the PA/urea mixture, three novel impurity compounds (I, II, III) were identified (**Figure S.8**). To further understand the impurity formation schemes, neat [1-^{13}C]PA and 10M [^{13}C, ^{15}N$_2$]urea solution were mixed at a 4:1 molar ratio, and dynamic ^{13}C NMR was acquired for 1 hour after the mixing. The spectra showed broad peaks, resulting from the high viscosity of the mixture and inefficient shimming due to the low D_2O concentration (**Figure S.9**). To identify these peaks, a gradual dilution was performed on this concentrated PA-urea mixture, where 50–100 µL of the approximately 700 µL solution was gradually replaced with D_2O, and ^{13}C spectra were taken after each dilution as shown in **Figure S.10**. As the sample becomes diluted, chemical shift changed due to concentration, pH, and solvent changes. As shimming quality improved, PA and urea peaks became distinguishable. Based on the relative chemical shifts, previously unassigned peaks at 158 ppm and 173 ppm were assigned to Impurity I, and previously unassigned peaks at 155 ppm and 174 ppm were assigned to Impurity II (**Figure S.10**).

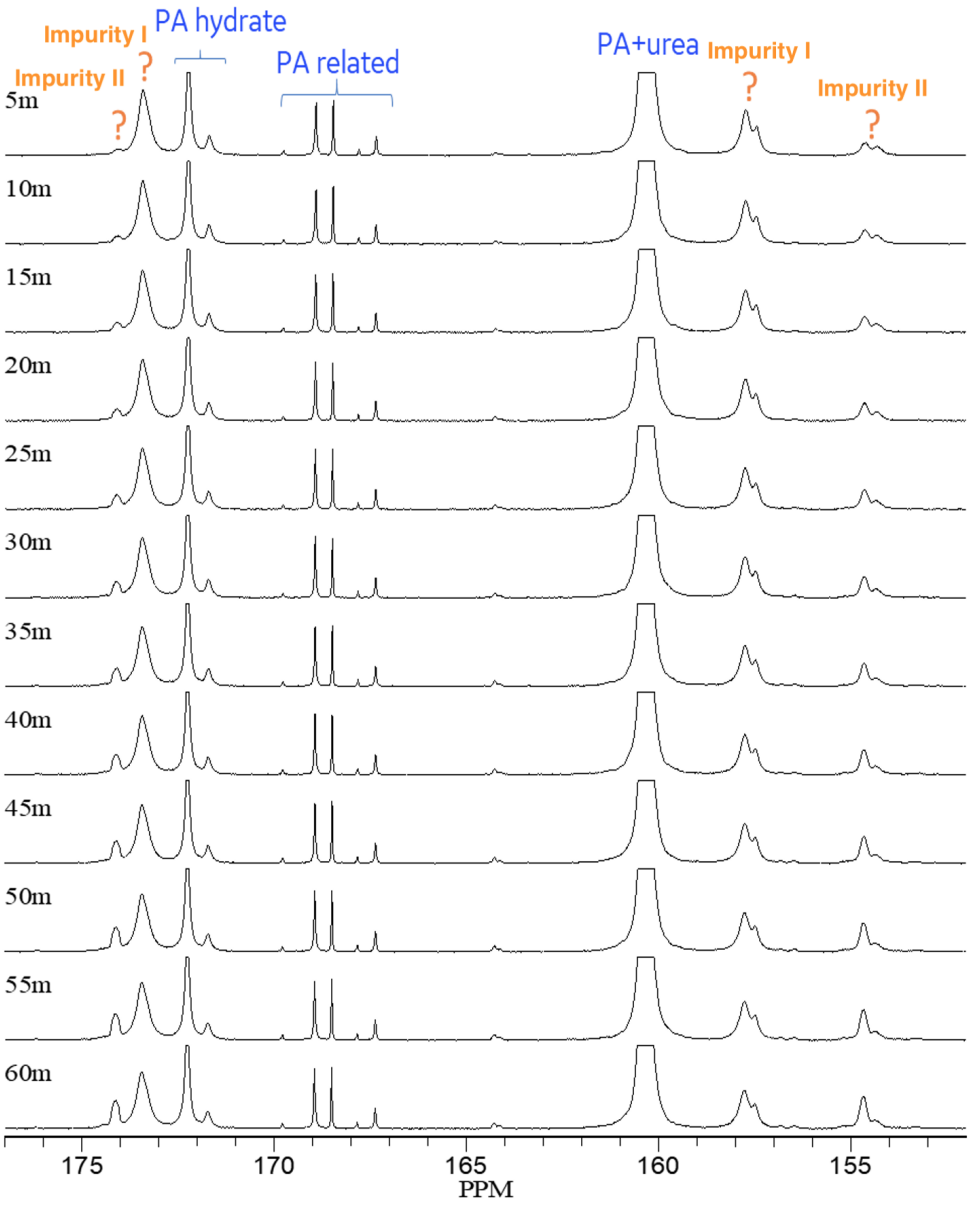

Figure S.9: Dynamic ^{13}C spectra of [1-^{13}C]pyruvic acid and [^{13}C,$^{15}N_2$]urea mixture at high concentration to demonstrate impurities are formed in starting material. Peaks marked with "?" could not be resolved in this experiment due to broad line width, but they were identified in the subsequent D_2O experiments as Impurity I and II. The dynanmic spectra show that impurity I forms rapidly in the cryovial upon the mixing of pyruvic acid and urea, whereas Impurity II forms slowly.

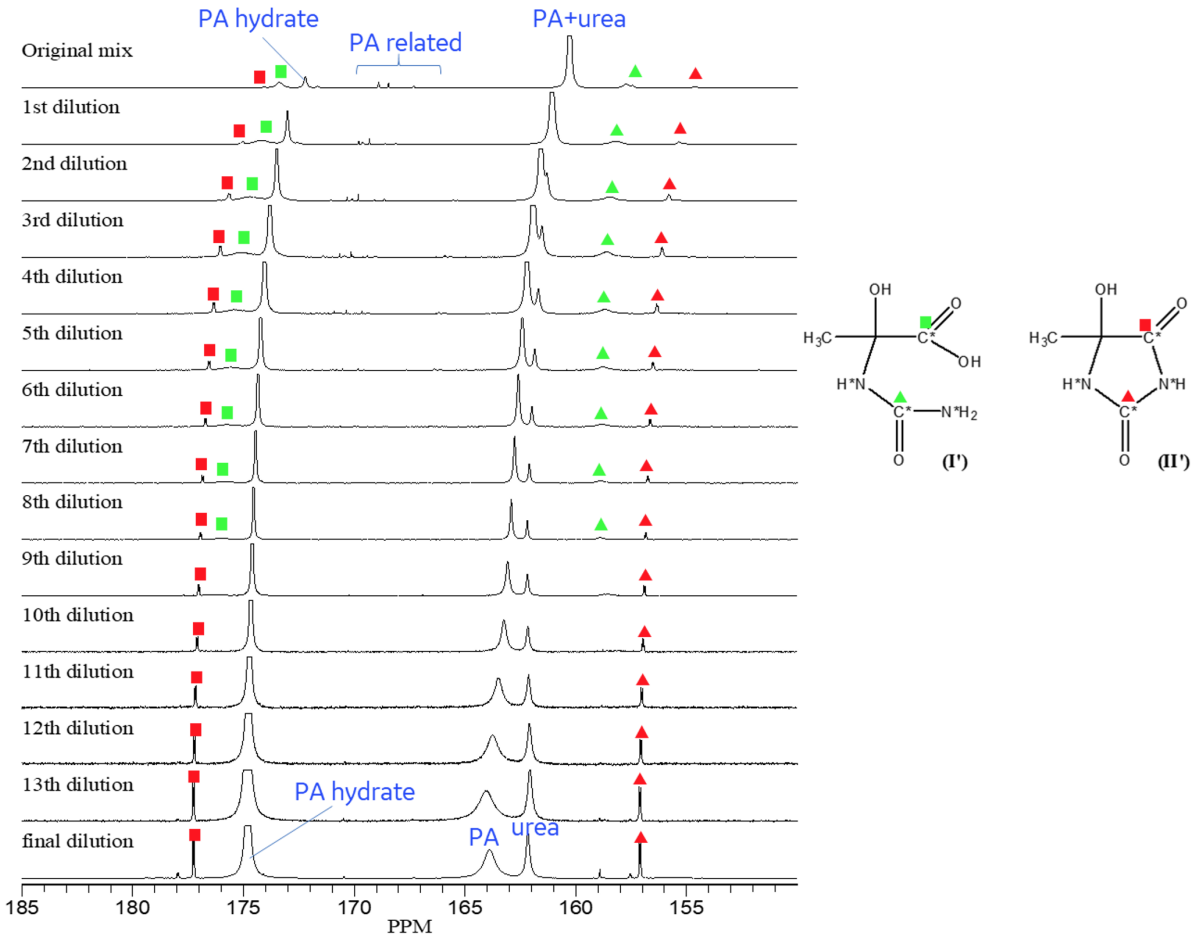

Figure S.10: ^{13}C spectra of [1-^{13}C]pyruvic acid (PA) and [^{13}C,^{15}N$_2$]urea starting material (cryovial conditions) as being gradually diluted with D_2O showed Impurity I peaks gradually disappear while Impurity II peaks gradually enhance, suggesting that Impurity I is readily converted to Impurity II at lower concentrations.

Taken together, the dynamic ^{13}C NMR of high concentration starting material and its gradual dilution suggest that Impurity I forms rapidly in the cryovial upon the mixing of pyruvic acid and urea, whereas Impurity II forms slowly. However, Impurity I is readily converted to Impurity II upon dissolution. Impurity III was not observed in this set of NMR experiments.

Further ^{13}C NMR studies were performed on the post-dissolution SPINlab Pharmacy Kit cryovial residual sample to confirm that the novel impurities identified by bench-top experiments also present in the actual SPINlab dissolution DNP experiments. Additionally, [1-^{13}C]pyruvic acid and [^{13}C,^{15}N$_2$]urea have longer cross-reaction time in the post-dissolution cryovial (up to 3 hours)

than bench-top studies, yielding higher impurity concentration that allows better elucidations of their structures (**Figure S.11**). Notably, Impurity I was not observed in SPINlab Pharmacy Kit cryovial.

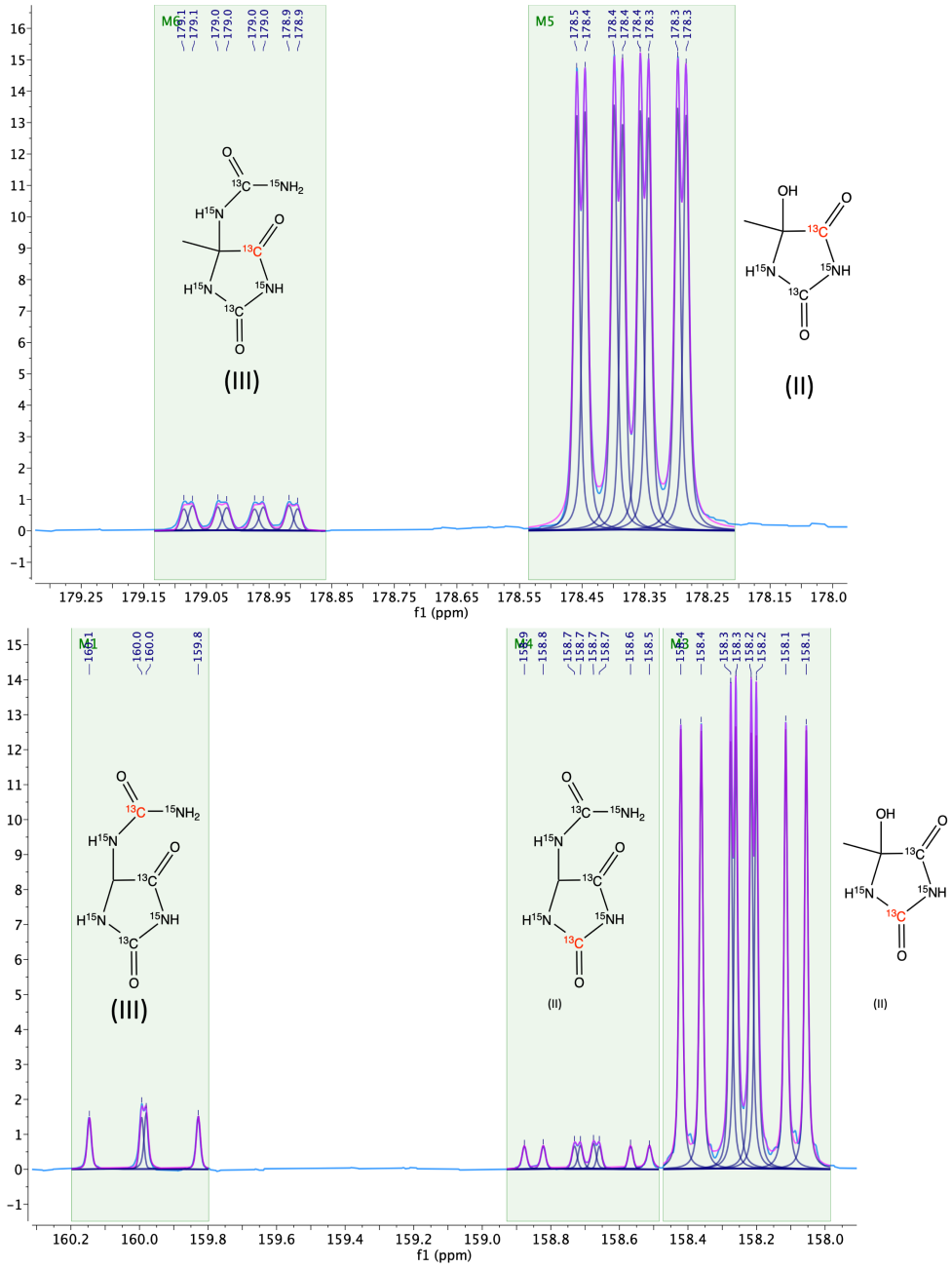

Figure S.11: ^{13}C NMR spectra of post-dissolution SPINlab Pharmacy Kit cryovial residual sample (high impurity content due to long reaction time and high concentration condition) shows the unique coupling content and the relative concentration of Impurity II and III. Impurity I was not observed in the post-dissolution cryovial.

Finally, impurity levels were quantified in the dissolution of [1-^{13}C]pyruvic acid and [^{13}C,^{15}N$_2$]urea. A bench-top manual dissolution was performed to replicate the Pharmacy Kit preparation process (including mixing, freezing, and thawing the starting material) and the SPINlab automated dissolution process (with rapid temperature and pH changes) (**Figure S.12**). The manual dissolution was performed adjacent to analytic instruments to minimize the sample transfer time and to mimic the patient injection time scale. The target concentration for manual dissolution was 200 mM [1-^{13}C]pyruvic acid and 50 mM [^{13}C,^{15}N$_2$]urea. Quantitative ^{13}C NMR spectra were collected immediately after dissolution for 1 hour with 8 minutes scan time per spectra (**Figure S.13**). The impurity information is summarized in **Table S.3**, and the NMR data was used to guide the LC-MS analyses and quantifications.

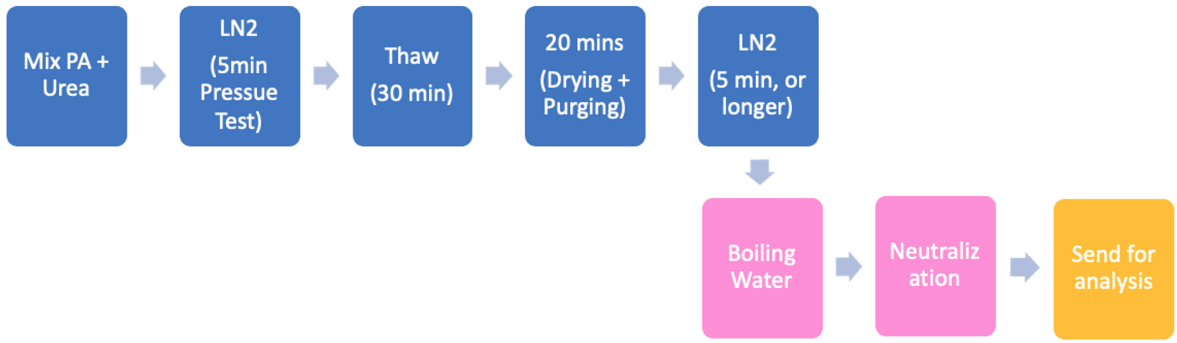

Figure S.12: Flowchart of the manual dissolution experiment to replicate SPINlab Pharmacy Kit preparation process (top row) and SPINlab polarizer dissolution process (bottom row). [1-^{13}C]pyruvic acid (PA) and [^{13}C, ^{15}N$_2$]urea are mixed at room temperature and then placed in liquid nitrogen (LN$_2$) for 5 minutes to replicate SPINlab Pharmacy Kit pressure test in LN$_2$. The sample is subsequently thawed at room temperature for 50 minutes to simulate the thawing, drying, and purging procedures of SPINlab Pharmacy Kit, followed by placing the sample into LN$_2$ again to simulate loading the sample into the SPINlab polarizer. Then, the frozen sample is rapidly dissolved in boiling water (100°C), to simulate Part A dissolution syringe, and subsequently mixed with neutralization media consisting of NaOH, Tris, and EDTA to simulate Part B receiver vessel neutralizations. The dissolved and neutralized sample was sent for LC-MS and NMR analysis immediately. The sample used for NMR analysis was dissolved by boiling D$_2$O to improve spectra resolution and quality.

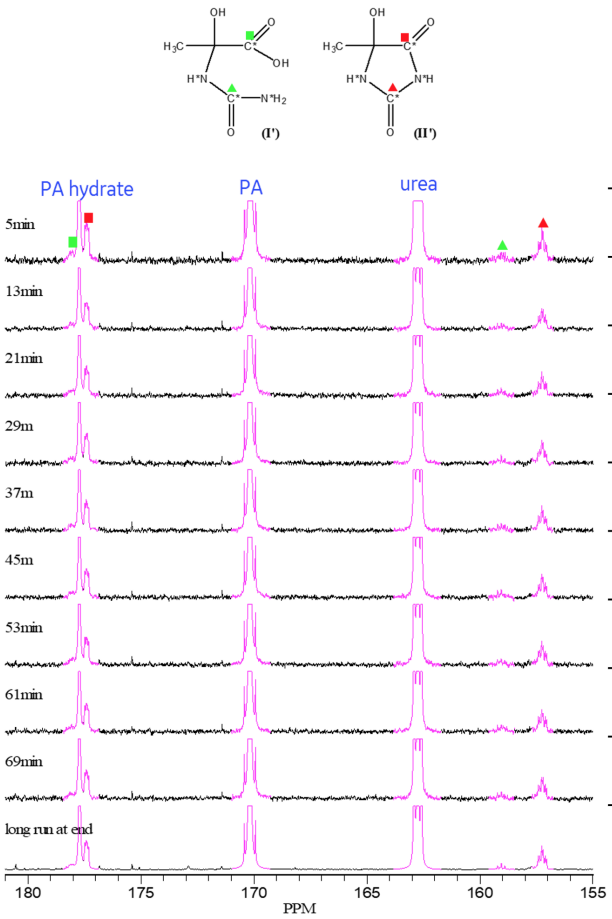

Impurity I	Impurity II
0.5%	2.0%
0.5%	1.8%
0.5%	1.9%
0.4%	1.7%
0.5%	1.9%
0.5%	1.8%
0.4%	1.8%
0.6%	1.9%
0.3%	1.7%
0.3%	1.7%

Figure S.13: Dynamic ^{13}C NMR spectra of manual dissolution product of [1-^{13}C]pyruvic acid and [^{13}C,$^{15}N_2$]urea with the corresponding % molar concentration of Impurity I and II. Impurity I and II concentrations are stable within one-hour post-dissolution.

Table S.3: Structure and characterization of novel impurities in co-polarized [1-^{13}C]pyruvate and [^{13}C,^{15}N$_2$]urea

Assigned name	Chemical Structure	Chemical nomenclature	Molecular formula	Mole % in the injection product	J coupling constant
Impurity I	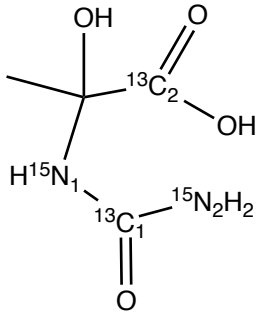	2-hydroxy-2-[^{13}C,^{15}N$_2$]ureido-[1-^{13}C]propanoic acid	$C_2{}^{13}C_2H_8{}^{15}N_2O_4$	0.5%* by NMR; not detected by LCMS (*near equipment detection limits)	$J_{CC} = 0.8$ Hz $J_{C1N1} = 19.6$ Hz $J_{C1N2} = 20$ Hz
Impurity II	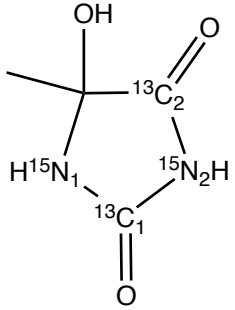	5-hydroxy-5-methyl-[2,4-^{13}C, 1,3-^{15}N]hydantoin	$C_2{}^{13}C_2H_6{}^{15}N_2O_3$	1.71 ± 0.26% by LCMS; 2% by NMR	$J_{CC} = 7.5$ Hz $J_{C1N1} = 18.3$ Hz $J_{C1N2} = 20.2$ Hz $J_{C2N1} = 1.7$ Hz $J_{C2N2} = 12.7$ Hz
Impurity III	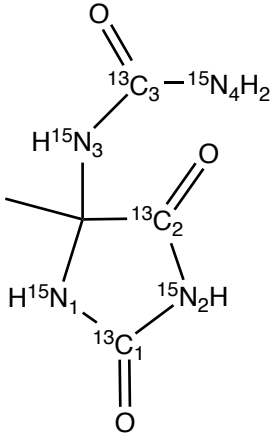	5-methyl-5-[^{13}C,^{15}N$_2$]ureido-[2,4-^{13}C, 1,3-^{15}N]hydantoin	$C_2{}^{13}C_3H_8{}^{15}N_4O_3$	0.48 ± 0.12% by LCMS; not detected by NMR	$J_{C1C2} = 6.9$ Hz $J_{C1N1} = 18.3$ Hz $J_{C1N2} = 20.5$ Hz $J_{C2N1} = 1.7$ Hz $J_{C2N2} = 14.2$ Hz $J_{C3N3} = 20.9$ Hz $J_{C3N4} = 19.2$ Hz

IV. LC-MS Methods and Results

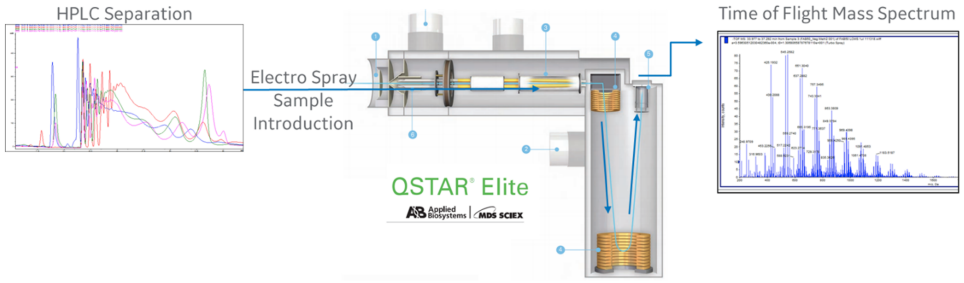

Figure S.14: Workflow of Liquid chromatography–mass spectrometry (LC-MS) study. Reversed-phase HPLC was run through Scherzo SS-C18 2 mm × 75 mm (Imtakt, Portland, OR) column at a flow rate of 0.2 ml/min using gradient elution with Solvent A (99.99% deionized water; 0.1% formic acid) and Solvent B (99.99% acetonitrile; 0.1% formic acid) under the following conditions: 0-5 minutes (100% Solvent A), 5-15 minutes (0-100% Solvent B), and 10 minutes equilibration to initial condition.

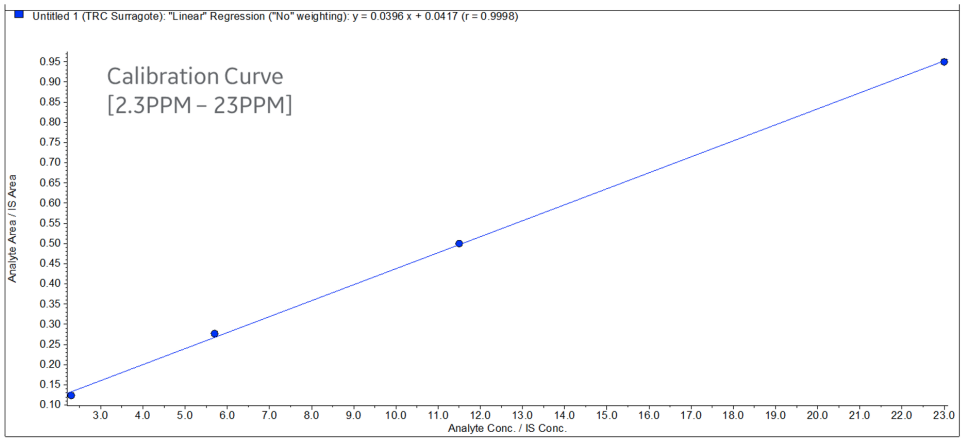

Figure S.15: LC-MS concentration quantification calibration curve using an internal reference standard of Impurity II (5-hydroxy-5-methyl-hydantoin).

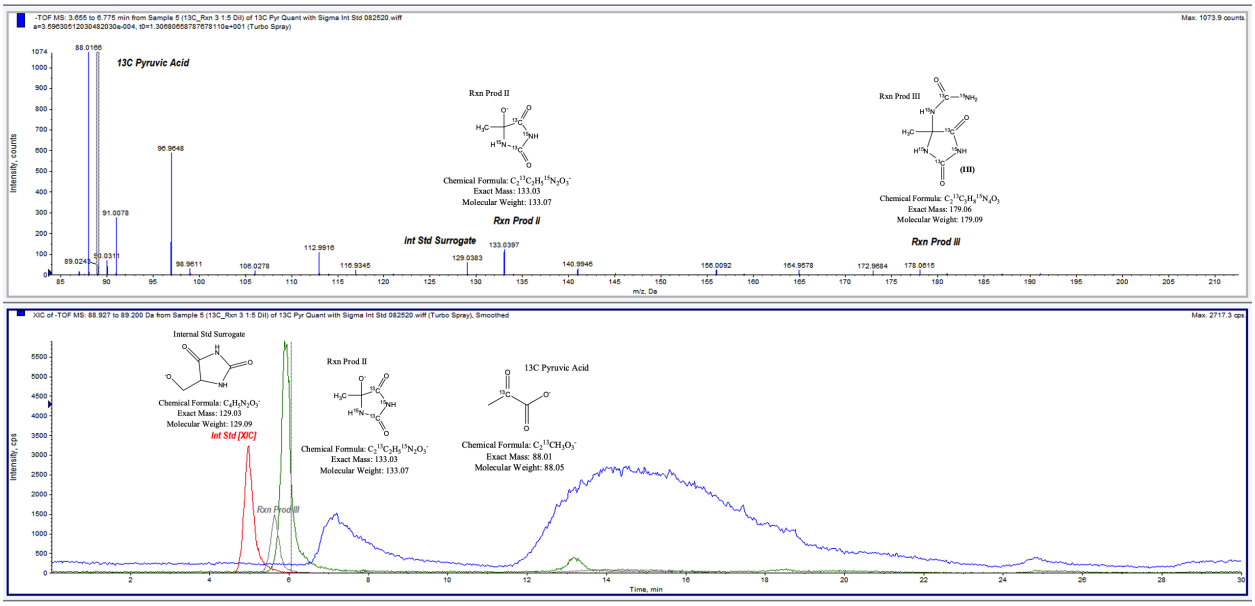

Figure S.16: Top figure shows a representative negative ion (red) Time of Flight (TOF) Mass Spectra (MS) overlays for the [1-^{13}C]pyruvic acid, [^{13}C, ^{15}N]urea, and Impurity II and III, with their expected mass-charge ratio. Bottom figure shows a representative negative ion extracted ion chromatogram (XIC) of [^{13}C, ^{15}N]urea and [1-^{13}C]pyruvic acid along with Impurity II and III.

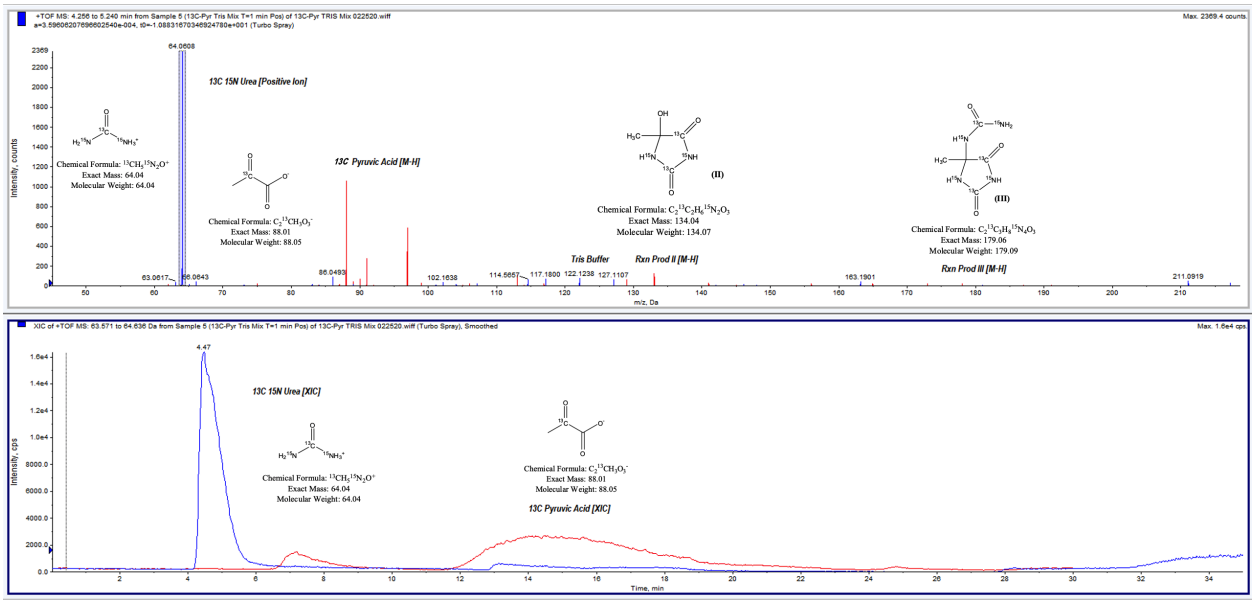

Figure S.17: Top figure shows a representative positive ion (blue) and negative ion (red) Time of Flight (TOF) Mass Spectra (MS) overlays for the [1-^{13}C]pyruvic acid, [^{13}C, ^{15}N]urea, along with impurities. Bottom figure shows a representative positive ion (blue) and negative ion (red) extracted ion chromatogram (XIC) of [^{13}C,^{15}N]urea and [1-^{13}C]pyruvic acid observed in the mixture. The quantitative analysis of all components required the positive ionization for [^{13}C, ^{15}N]urea. All other compounds were quantified by negative ionization, which produces little solvent adducts.

V. Toxicology study data

Four groups of male Sprague-Dawley rats (2-3 months old, 0.4-0.55 kg body weights) were intravenously injected with 2.5 ml of the following solution over 10 s: (I) saline control, n = 3; (II) HP co-polarized injection product (approximately 150 mM pyruvate, 35 mM urea), n = 10; (III) Impurity II (5-hydroxy-5-methyl-hydantoin; 40 mM in saline), n = 5; (IV) Impurity III (5-methyl-5-ureido-hydantoin; 20 mM in saline), n = 5. All numerical data in this section are reported at mean ± standard deviations. (Abbreviations: Co-Pol, co-polarized [1-^{13}C]pyruvate and [^{13}C,^{15}N$_2$]urea.)

Table S.4: Heart rate during injection (bpm)

Group	Injection	Baseline	5 min	10 min	15 min	20 min
I	Saline control	273 ± 16	279 ± 14	277 ± 10	280 ± 9	282 ± 21
II	Co-Pol	309 ± 43	314 ± 30	320 ± 30	324 ± 29	326 ± 28
III	Impurity II	316 ± 36	336 ± 28	334 ± 30	336 ± 31	337 ± 36
IV	Impurity III	337 ± 54	340 ± 31	348 ± 29	342 ± 36	344 ± 20

Table S.5: Breath rate during injection (bpm)

Group	Injection	Baseline	5 min	10 min	15 min	20 min
I	Saline control	39 ± 7	38 ± 5	39 ± 6	41 ± 8	41 ± 8
II	Co-Pol	42 ± 10	45 ± 9	46 ± 8	45 ± 8	47 ± 10
III	Impurity II	50 ± 11	54 ± 9	55 ± 13	54 ± 10	57 ± 8
IV	Impurity III	60 ± 5	55 ± 4	56 ± 13	54 ± 7	57 ± 9

Table S.6: Oxygen saturation during injection (%)

Group	Injection	Baseline	5 min	10 min	15 min	20 min
I	Saline control	99.5 ± 0.2	99.5 ± 0.1	99.5 ± 0.1	99.4 ± 0.1	99.5 ± 0.2
II	Co-Pol	98.9 ± 1.0	98.9 ± 0.9	98.9 ± 0.8	98.9 ± 0.9	99.0 ± 0.6
III	Impurity II	99.3 ± 0.7	99.5 ± 0.2	99.4 ± 0.4	99.3 ± 0.5	99.1 ± 0.5
IV	Impurity III	99.6 ± 0.2	99.6 ± 0.3	99.6 ± 0.3	99.6 ± 0.3	99.6 ± 0.1

Table S.7: Body weights 2 weeks post-injection (kg)

Group	Injection	SD1	SD3	SD5	SD8	SD10	SD13	SD15
I	Saline control	0.47	0.48	0.48	0.48	0.49	0.50	0.50
II	Co-Pol	0.47	0.47	0.47	0.48	0.48	0.48	0.49
III	Impurity II	0.47	0.47	0.47	0.47	0.48	0.48	0.48
IV	Impurity III	0.50	0.49	0.49	0.50	0.50	0.50	0.51

Abbreviation: SD, study day

Table S.8: Complete Blood Count (CBC) at baseline, 20 minutes, and 2 weeks post-injection

Test	Group I: Saline control (n = 3)			Group II: Co-Pol (n = 10)			Group III: Impurity II (n = 5)			Group IV: Impurity III (n = 5)			Reference range
	baseline	20 min	2-week	baseline	20-min	2-week	baseline	20-min	2-week	baseline	20-min	2-week	
WBC (1000 cells/uL)	12.7 ± 1.5	9.2 ± 3.1	11.7 ± 2	10.97 ± 1.35	9.3 ± 3.03	8.43 ± 2.13	9 ± 0.8	6.8 ± 1.8	6.9 ± 1.6	9.6 ± 1.1	6.9 ± 1.4	9.9 ± 0.6	6.0–18.0
Neut%	19 ± 4.6	21.5 ± 6.8	20.4 ± 3.2	20 ± 4.6	27.3 ± 5.2	20.9 ± 6	22.2 ± 8.7	34 ± 14	20.4 ± 3.5	20.8 ± 3.6	32.7 ± 7.2	21.1 ± 3.1	10.0–30.0
Lymp%	75.4 ± 5.8	72.8 ± 6.9	74.1 ± 4.7	66.4 ± 21.1	64.4 ± 5.4	73.4 ± 6.9	71.7 ± 9	56.7 ± 16.6	73.4 ± 3	72.3 ± 4.1	57 ± 9.9	72.7 ± 4.2	65.0–85.0
Mono%	4.3 ± 0.9	5.3 ± 0.8	4.5 ± 0.7	4.88 ± 0.87	6.67 ± 2.11	4.04 ± 1.66	4.2 ± 1.6	6.7 ± 3	3.9 ± 1.9	4.9 ± 1.1	8.6 ± 2.5	4.2 ± 0.3	0.0–5.0
Eos%	0.8 ± 0.2	0.4 ± 0.4	0.7 ± 0.8	1.43 ± 0.95	1.37 ± 0.85	1.17 ± 0.98	1.7 ± 1.4	2.2 ± 1.5	1.7 ± 0.2	1.7 ± 0.9	1.6 ± 1.2	1.4 ± 0.5	0.0–6.0
Baso%	0.5 ± 0.2	0.1 ± 0.1	0.7 ± 0.3	0.22 ± 0.18	0.24 ± 0.24	0.52 ± 0.48	0.2 ± 0.1	0.5 ± 0.7	0.5 ± 0.2	0.4 ± 0.5	0.2 ± 0.2	0.6 ± 0.3	0.0–1.0
HGB (g/dL)	15.4 ± 0.9	14.5 ± 0.4	14.6 ± 1.4	15.2 ± 1.5	13.4 ± 1.2	14.9 ± 1.9	16.2 ± 0.8	14.8 ± 0.3	15.4 ± 0.9	15.7 ± 0.7	14.6 ± 0.7	15.1 ± 0.2	9.2–11.0
HCT (%)	46.1 ± 4	42.7 ± 0.5	44.2 ± 0.9	44.4 ± 2.3	40.8 ± 2.9	42.8 ± 3.6	45.9 ± 2.7	42.7 ± 1.1	43.7 ± 2.4	44.5 ± 2.8	41.8 ± 2.2	42.9 ± 0.5	36.0–54.0
PLT (1000 cells/uL)	971 ± 161	1125.3 ± 430.2	1363.7 ± 299.4	1109 ± 146	982 ± 151	735 ± 226	1084.6 ± 77.9	996 ± 168.1	848.8 ± 156.3	1084.6 ± 77.9	996 ± 168.1	848.8 ± 156.3	300–500

Abbreviations: WBC, white blood cells; Neut, neutrophils; Lymp, lymphocytes; Mono, monocytes; Eos, eosinophils; Baso, basophils; HGB, hemoglobin; HCT, hematocrit; PLT, platelet count.

N.B. Reference ranges for rats were provided by UC Davis Comparative Pathology Laboratory. Group I saline control serves as additional reference to account for species and age.

Table S.9: Liver-kidney (L-K) panel at baseline, 20 minutes, and 2 weeks post-injection

Test	Group I: Saline control (n = 3)			Group II: Co-Pol (n = 10)			Group III: Impurity II (n = 5)			Group IV: Impurity III (n = 5)			Reference range
	baseline	20 min	2-week	baseline	20-min	2-week	baseline	20-min	2-week	baseline	20-min	2-week	
ALT (U/L)	28.5 ± 4.1	27.1 ± 3.9	29.5 ± 2.8	45.1 ± 18.4	31.9 ± 6.3	30.5 ± 6.3	33.5 ± 5.2	30.7 ± 2.8	30.5 ± 3.5	34.8 ± 4.6	31.6 ± 4.7	34.1 ± 2.8	12–67
AST (U/L)	59.6 ± 15.9	64.4 ± 29.4	68 ± 7.7	72.8 ± 22.6	62.2 ± 11.9	55.3 ± 13	61.4 ± 3.8	60.3 ± 3.8	55.6 ± 3.7	68 ± 7.9	67 ± 5.6	61.8 ± 3.4	14–113
ALB (g/dL)	4 ± 0.1	3.9 ± 0.1	3.9 ± 0.6	4.1 ± 0.2	3.6 ± 0.2	2.8 ± 0.2	3.9 ± 0.1	3.6 ± 0.2	3.8 ± 0.2	3.9 ± 0.1	3.6 ± 0.2	3.8 ± 0.1	2.7–4.6
Alk Phos (U/L)	106 ± 1.2	106.1 ± 4	107.1 ± 12	179.5 ± 36.1	152 ± 25	114.6 ± 32.4	143.6 ± 15.5	125.6 ± 20.5	124.9 ± 15.4	153.7 ± 21.8	136.1 ± 18.1	139.9 ± 25.4	136–188
BUN (mg/dL)	14.5 ± 1.1	19.7 ± 3.3	16.7 ± 4.6	16.2 ± 1.8	18.7 ± 2.2	13.6 ± 1.8	17.9 ± 3.2	19.8 ± 3.3	20 ± 4.2	16.9 ± 2.2	18.6 ± 2.6	19.3 ± 1.7	10–25
Cr (mg/dL)	0.23 ± 0.02	0.25 ± 0.03	0.29 ± 0.05	0.3 ± 0.03	0.3 ± 0.05	0.2 ± 0.04	0.31 ± 0.04	0.31 ± 0.05	0.28 ± 0.05	0.33 ± 0.01	0.31 ± 0.01	0.3 ± 0.03	0.8–1.8
TBIL (mg/dL)	0.066 ± 0.005	0.062 ± 0.033	0.126 ± n.a.	0.028 ± 0.019	0.035 ± 0.025	0.028 ± 0.022	0.026 ± 0.016	0.042 ± 0.009	0.05 ± 0.018	0.037 ± 0.018	0.021 ± 0.023	0.059 ± 0.029	0.2–0.7
TP (g/dL)	5.7 ± 0.5	5.5 ± 0.3	5.7 ± 0.4	5.8 ± 0.2	5.1 ± 0.3	4 ± 0.2	5.6 ± 0.1	5.2 ± 0.3	5.4 ± 0.3	5.6 ± 0.2	5.2 ± 0.3	5.6 ± 0.2	5.3–7.5

Abbreviations: ALT, alanine aminotransferase; U/L, international unit/L; AST, aspartate aminotransferase; ALB, Albumin; Alk Phos, alkaline phosphatase; BUN, blood urea nitrogen; Cr, Creatinine; TBIL, Total Bilirubin; TP, Total protein.
N.B. Reference ranges for rats were provided by UC Davis Comparative Pathology Laboratory. Group I saline control serves as additional reference to account for variations in species and age.

VI. Urea-specific RF pulse design

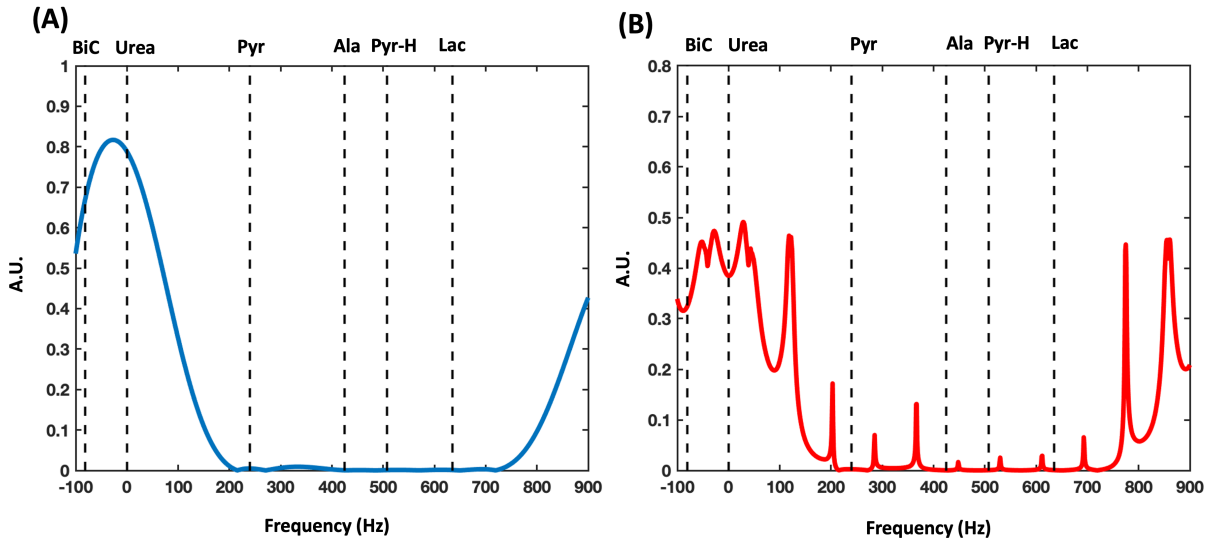

Figure S.18: (A) The excitation spectral profile of the ^{13}C urea frequency-specific, non-spatially selective RF pulse shows that the ^{13}C urea resonance (referenced at 0 Hz) is targeted by the RF pulse with minimal perturbations to ^{13}C pyruvate, alanine, pyruvate hydrate, and lactate (dash lines). However, the ^{13}C bicarbonate resonance is also excited by this RF pulse, limiting its application to organs or diseases where the bicarbonate signal is negligible. (B) The transverse magnetization responses of the urea-specific balance steady-state free precession (bSSFP) sequence show no overlaps between spectral banding artifacts (peaks outside the urea spectral region) and resonance frequencies of metabolites of interests (dash lines). The RF pulse was designed using Spinbench software, and the simulation and visualization was performed using MATLAB. Abbreviations: BiC, bicarbonate; Pyr, pyruvate; Ala, alanine; Pyr-H, pyruvate hydrate; Lac, lactate.